

Exploring inertial effects in the flow of granular media: double-scale approach MPM×DEM

Viet Anh Quach¹, Olivier Ozenda², Guillaume Chambon², Gaël Combe^{1,*}, and Vincent Richefeu^{1,**}

¹Univ. Grenoble Alpes, CNRS, Grenoble INP, 3SR, 38000 Grenoble, France.

²Univ. Grenoble Alpes, CNRS, INRAE, IRD, Grenoble INP, IGE, 38000 Grenoble, France.

Abstract. In the exploration of cohesive granular materials, one challenge lies in the significant impact of microstructure evolution on the system's overall mechanical behavior, which necessitates the consideration of a broad spectrum of scales. To address this, a hierarchical double-scale approach that combines MPM (Material Point Method) and DEM (Discrete Element Method) has been introduced. The MPM solver, responsible for large-scale flow, uses a Computationally Homogenized Constitutive Law (CHCL) derived from the resolution of numerous individual DEM problems at each material point. The DEM cells are three-periodic and incorporate standard frictional contact laws between the elements. This work focuses mainly on the unique aspects of the two-way coupling strategy between these two numerical methods, with particular emphasis on coordinating the explicit MPM and DEM time steps to ensure computational stability. Preliminary benchmark simulations of the collapse of a cohesive column are presented, with emphasis on the inertial aspects enabled by the dynamic nature of MPM and DEM.

1 Introduction

Cohesive granular materials are found in natural and industrial processes, such as landslides, avalanches, and powder handling. Their mechanical behavior is highly complex due to interactions at the grain scale, including contact evolution, bond breakage, and microstructural changes. Traditional continuum approaches struggle to capture these effects accurately. We present a multi-scale modeling approach using the Material Point Method (MPM) for macroscopic flow and the Discrete Element Method (DEM) for grain-scale interactions. This hierarchical coupling ensures that large-scale material response is informed by physically-based microscale mechanisms.

This approach builds on existing ideas, but the innovative aspect we highlight in this brief paper is that both the MPM at the macroscopic level and the DEM at the grain level can handle inertial effects. The concept behind this hierarchical model is to use small-scale direct simulations to develop a Computationally Homogenized Constitutive Law (CHCL) concurrently with the computational operations. Incorporating rate dependency into this law would further enhance its effectiveness.

2 Methodology

2.1 MPM as a dynamic macroscopic solver

Since pioneering work of Sulsky *et al.* (1994) [1], many variants of the Material Point Method (MPM) have been

developed. This study assumes familiarity with MPM principles. We use a 2D MPM algorithm based on Gracia *et al.* (2019) [2] and implemented in an in-house software [3] hosted on GitHub. In a nutshell, MPM discretizes the governing equations over moving material points while solving them on a fixed background grid. The weak form of the momentum conservation equation is given by:

$$\int_{\Omega} \left(\rho \frac{dv}{dt} \cdot w^* \right) d\Omega = \int_{\Omega} (-\rho \sigma : \nabla w^* + \rho g \cdot w^*) d\Omega. \quad (1)$$

The implementation employs the Modified Update Stress Last (MUSL) scheme for time integration, chosen for its stability over standard methods. Numerical dissipation is controlled via a FLIP-PIC interpolation, balancing accuracy and convergence by adjusting a weighting parameter. To mitigate cell crossing instability, cubic B-splines are used for interpolation instead of GIMP-based methods.

Boundary conditions are enforced using a DEM-like contact law, with rigid edges interacting elastically and frictionally with material points modeled as disks. In the MPM scheme, these frictional contact forces are considered as external boundary forces. Stability is ensured through a critical time step computed from multiple criteria, including CFL conditions, material point overlap, and rigid body interactions. Additional stability considerations for the MPM×DEM framework are introduced later.

2.2 Periodic DEM as an homogenized law

At each MPM time step, a transformation increment is applied to a DEM cell, whose mechanical response must be

*e-mail: gael.combe@univ-grenoble-alpes.fr

**e-mail: vincent.richefeu@univ-grenoble-alpes.fr

representative of the surrounding material while minimizing edge effects, achieved through tri-periodic boundary conditions. Following the approach of Allen and Tildesley (1987) [4] for molecular dynamics and its extension to Lagrangian models by Radjai and Voivret (2011) [5], the periodic cell is defined by a matrix \mathbf{h} composed of three vectors that describe its nine degrees of freedom. This matrix represents the *combined degrees of freedom* dictated by the transformation increment from the MPM.

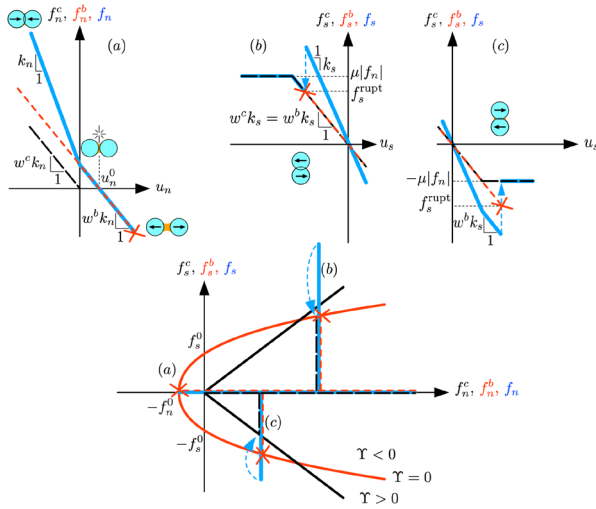


Figure 1. Illustration of force laws between rigid spherical particles, neglecting viscous forces and using stiffness weights $w_c = w_b = 1/2$. (a) Normal force combines elastic contact repulsion and bond force canceling u_n^0 . (b), (c) Tangential force includes friction (if in contact) and shear bond resistance. (Bottom) Bonds and Coulomb yield surfaces in (f_n, f_s) space, with yield functions for bond breakage (red) and friction (black). Dashed black: contact forces; dashed red: bond forces; solid blue: resultants; blue dashed arrows: force jumps at bond breakages.

We use a simplified interaction law from [6], omitting bond damage, where forces result from visco-damped frictional contacts and elastic-fragile bonds. The interaction forces depend on two state variables: Ψ^c for contact and Ψ^b for bond presence, influencing normal and tangential stiffness. Normal force comprises elastic, viscous, and bond components, while tangential force accounts for Coulomb friction and bond shear resistance. Bond rupture follows a yield function, with different failure modes illustrated in Figure 1. After bond failure, contact and friction forces persist if active, distinguishing bond and contact mechanics. For brevity, the mathematical expressions of the force laws and yield function are not detailed here.

3 Communication across scales

In the hierarchical MPM×DEM model, each MPM time step Δt^{MPM} queries a periodic DEM cell, deforms it at a rate $\dot{\mathbf{h}}$, and retrieves the homogenized Cauchy stress *via* computational homogenization constitutive law (CHCL), as shown in Figure 2. The DEM uses explicit time steps δt , ensuring $\Delta t^{\text{MPM}} = \sum \delta t$.

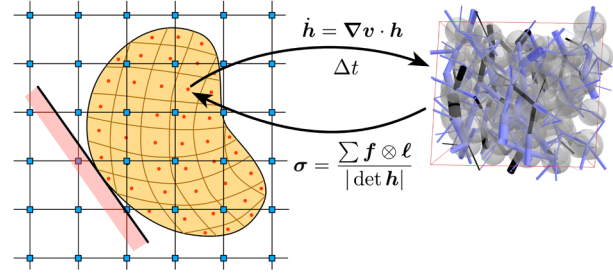


Figure 2. Relations across scales in a hierarchical MPM×DEM model. Each material point links to a periodic DEM cell, queried by $\nabla \mathbf{v}$ over duration Δt^{MPM} , returning the average Cauchy stress *via* Love-Weber homogenization (shown without kinetic term here).

The stress tensor is computed as:

$$\sigma_p = \frac{-1}{|\det \mathbf{h}_p|} \left(\sum_k \mathbf{f}_k \otimes \boldsymbol{\ell}_k + \sum_n m_n \dot{\mathbf{r}}_n \otimes \dot{\mathbf{r}}_n \right) \quad (2)$$

where the first term denotes Love-Weber stress, while the second (kinetic) term may become significant during extremely rapid deformations.

Both MPM and DEM remain dynamic, capturing strain-rate effects. To maintain physical consistency, the density at the material point evolves with its DEM volume change: $|\det \mathbf{h}_p|$. Stability conditions ensure $\delta t < \Delta t^{\text{MPM}}$, with:

$$\delta t = Q_t \pi \sqrt{\frac{k_n}{m_{\min}}} \quad \text{and} \quad \delta t \leq \frac{\Delta t^{\text{MPM}}}{Q_n} \quad (3)$$

where Q_t and Q_n regulate DEM time stepping. Additionally, to limit excessive deformations, the MPM time step must satisfy:

$$\Delta t^{\text{MPM}} = Q_h \frac{d_{\min}}{|\dot{\mathbf{h}}_p|_{\text{sup}}} \quad (4)$$

where $|\dot{\mathbf{h}}_p|_{\text{sup}}$ is the largest component of the cell velocity in absolute value.

The careful handling of time stepping in both MPM and DEM is crucial for executing double-scale dynamic simulations. A challenging issue is determining which DEM stress should be transferred back to the MPM level, as the DEM cell can undergo significant stress fluctuations under rapid loading. To address this issue, a linear regression over the final fraction Q_σ of Δt^{MPM} provides a “stabilized” stress value to MPM (Figure 3).

Note, however, that this stress value is not statically stabilized but rather selected in such a way that it represents an appropriate value over the fluctuations occurring within the MPM time step. Consequently, some dynamic information within a single time step may be lost, but a certain level of dynamics is still preserved at the MPM scale. In practice, as demonstrated in the examples presented below, the stress stabilizes quickly at each time step because the loading is not yet sufficiently rapid (such as the impact of a projectile, for example). Nevertheless, we present this example to illustrate the ability of the approach to account for flow velocities at both scales.

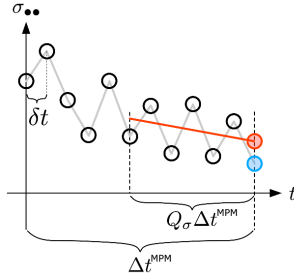


Figure 3. Schematic of computing homogenized stress σ_{ii} for a dynamic response over Δt^{MPM} . Black scatter: instantaneous DEM stress; red line: linear regression over the final fraction Q_σ ; red circle: interpolated value returned to MPM.

4 Application: dynamic column collapse

We simulate the collapse of a cohesive granular column with a height of 2.4 m. The material properties are calibrated to replicate snow-like behavior, with an average particle diameter of $370 \mu\text{m}$ and a density of 550 kg/m^3 . The column stabilizes under its self-weight before the collapse initiates. Figure 4 presents the material point velocity field at different stages, along with the DEM configurations both within and outside the shear band. The figure also illustrates the evolution of the elementary cells associated with two material points. The first cell is located in the upper central part of the column, while the second is positioned in the high-velocity-gradient zone (shear band) that develops during the flow. It is evident that the latter cell undergoes extreme distortion throughout the collapse, whereas the cell in the upper part primarily flattens, experiencing only minor direct shear deformation. Additionally, the number of cohesive bonds (represented by blue tubes) decreases significantly faster in the cell located in the shear band. Moreover, the deformation of the cells remains consistent with the overall shape evolution of the collapsing column over a relatively long period. This is highlighted by the absence of gaps between the shapes assigned to each material point (not shown). This consistency, which serves as a key indicator of the accuracy of the double-scale implementation, deteriorates as the cells become increasingly distorted. As a result, the simulations were stopped once the smallest cell dimensions approached the grain size, before the overall mass came to a complete halt, since the mechanical response provided by the CHCL was no longer representative.

Figure 5 illustrates the evolution of the deviatoric strain rate $\dot{\epsilon}_q$ and the damage D (the relative number of broken bonds) within the column. These two quantities are defined as follows:

$$\dot{\epsilon}_q = \sqrt{(\nabla v_{xx} - \nabla v_{yy})^2 + (\nabla v_{xy} + \nabla v_{yx})^2} \quad (5)$$

and

$$D(t) = 1 - \frac{N_b(t)}{N_b(0)} \quad (6)$$

where $N_b(t)$ represents the number of bonds at time t .

These two fields clearly highlight the accumulation of strain and damage in two inclined regions, which

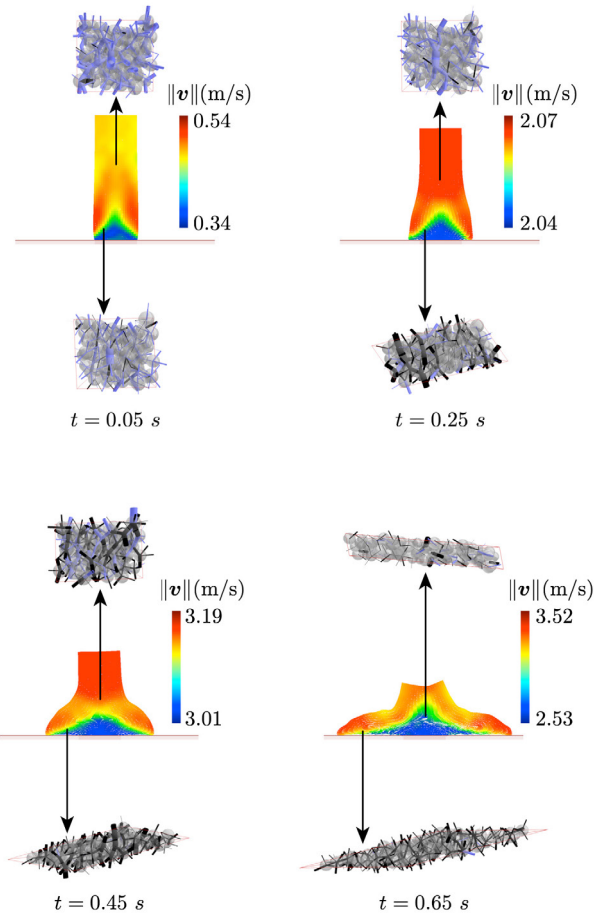


Figure 4. Collapse of the column at different times with the velocity norm represented by the color scale. The elementary cells associated with two selected material points are shown: one within the shear band and the other above it. The diameter of the blue (resp. black) tubes in the cells indicates the magnitude of cohesive (resp. purely frictional) interactions between spheres.

can be identified as shear bands. The localization of strain demonstrates that the model effectively captures the macroscopic softening behavior of the material through the progressive damage of its microstructure. Conversely, the low strain and damage values observed in the upper part of the column at early stages indicate a quasi-rigid motion. This region then begins to spread (see $t = 0.65$), yet the two initial top corners of the column remain distinguishable even in later phases of the collapse. Notably, this flow pattern is consistent with experimental observations reported by Gans [7] and with both continuous and discrete simulations presented in [8]. These latter studies also focused on dense cohesive granular materials.

5 Conclusion

This paper lays the foundation for a double-scale MPM×DEM model to simulate cohesive geophysical flows like avalanches and landslides. The main goal is to highlight subtle implementation challenges often overlooked in previous studies. A key advantage is that both

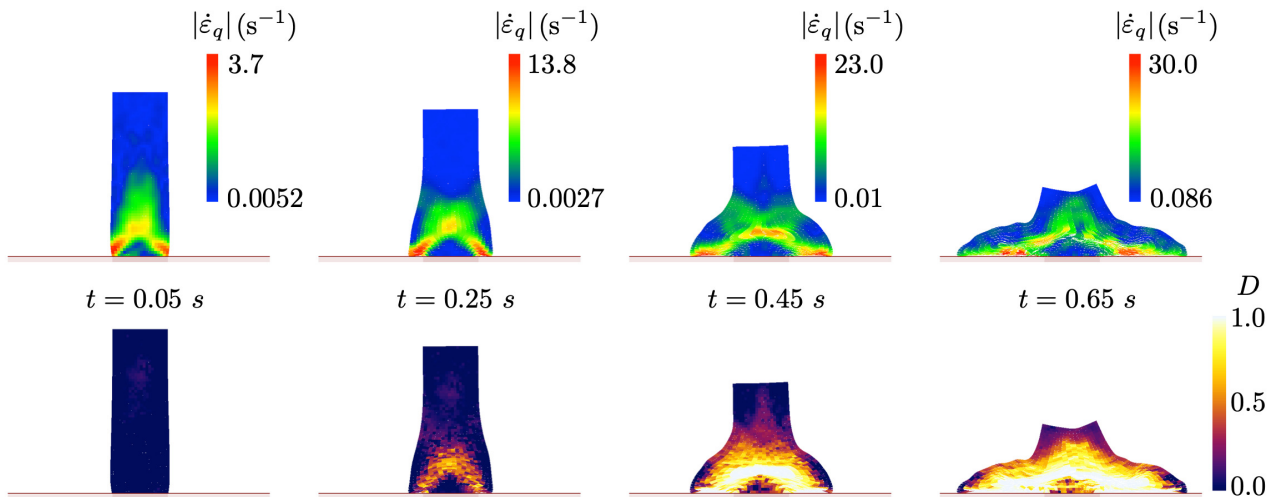


Figure 5. Evolution of deviatoric strain rate (top line) and damage (bottom line) inside the column at different times.

MPM and DEM codes are developed in-house, allowing precise control over model intricacies.

A novel aspect of this approach is using three-periodic DEM elementary volumes, where deformation increments from MPM are applied as an affine displacement field to DEM particles – unlike previous rigid boundary condition implementations. Additionally, dynamic effects are considered at both macro and micro scales, ensuring a consistent physical time framework. This differs from traditional hierarchical methods (*e.g.*, FEM×DEM), where macroscopic computations often ignore inertia. These model-specific features required introducing stability conditions and tuning time-step ratios for cross-scale communication.

Benchmark simulations of a collapsing dense cohesive granular column validated the method, focusing on DEM cell preparation and stabilization. Results revealed pronounced strain and damage accumulation at the column base, demonstrating that small-scale DEM periodic cells capture complex macroscopic mechanical behaviors. The independent microstructure evolution within DEM cells also led to spontaneous symmetry breaking in flow patterns.

Future work aims to enhance realism by incorporating grain polydispersity, non-spherical particles, and loose microstructures to better model real geomaterials like soil or snow. However, these additions may pose numerical stability challenges. Further improvements could also address mesh size dependence in MPM and excessive distor-

tions in DEM cells under high shear by employing modular transformation techniques.

Acknowledgements

This research has partly been supported by ANR project MiMESis-3D (ANR-19-CE01-0009).

References

- [1] D. Sulsky, Z. Chen, H.L. Schreyer, A particle method for history-dependent materials, *Compu. Meth. Appl. Mech. Eng.* **118**, 179 (1994).
- [2] F. Gracia, P. Villard, V. Richefeu, Comparison of two numerical approaches (dem and mpm) applied to unsteady flow, *Comput. Part. Mech.* **6**, 591 (2019).
- [3] V. Richefeu, G. Combe, MPM×DEM, <https://github.com/richefeu/mpmxdem> (2025)
- [4] M.P. Allen, D.J. Tildesley, in *Computer Simulation of Liquids*, edited by C. Press (Oxford University Press, New York, 1987), p. 182–211
- [5] F. Radjaï, C. Voivret, in *Discrete-element modeling of granular materials*, edited by F. Radjaï, F. Dubois (Wiley-Iste, London, 2011), pp. 181–198
- [6] C.B. Couture, Ph.D. thesis, Université Grenoble Alpes (2020)
- [7] A. Gans, Ph.D. thesis, Aix Marseille Université (2021)
- [8] A. Abramian, L. Staron, P.Y. Lagrée, The slumping of a cohesive granular column: Continuum and discrete modeling, *J. Rheol.* **64**, 1227 (2020).